Syntheses, Structures and Properties of a Cobalt(II) and a Cadmium(II) Complex Based on 1-((Benzotriazol-1-yl)methyl)-1*H*-1,3-imidazole and 1,3-Benzenedicarboxylate Ligands

Qiuying Huang[a,b], Weiping Tang[a], Yi Yang[a], and Wei Liu[a]

[a] Department of Chemical Engineering, Henan Polytechnic Institute, Nanyang, 473009, P. R. China

[b] The College of Chemistry and Molecular Engineering, Zhengzhou University, Zhengzhou 450001, P. R. China

Reprint requests to Prof. Qiuying Huang. E-mail: huangqy72@163.com

Z. Naturforsch. **2014**, *69b*, 423 – 431 / DOI: 10.5560/ZNB.2014-3297
Received October 25, 2013

Two new complexes with the formulae $\{[Co(bmi)_2(bdc)(H_2O)]\cdot 2H_2O\}_n$ (**1**) and $\{[Cd(bmi)(bdc)(H_2O)]\cdot DMF\}_n$ (**2**) (bmi = 1-((benzotriazol-1-yl)methyl)-1*H*-1,3-imidazole, H_2bdc = 1,3-benzenedicarboxylic acid) have been synthesized and characterized by single-crystal X-ray diffraction. Complex **1** exhibits a chain structure in which both carboxylate groups of each 1,3-benzenedicarboxylate coordinate to the Co(II) ions in monodentate and chelating modes, and the bmi ligands with a monodentate mode. Complex **2** features a layered structure where both carboxylate groups of each 1,3-benzenedicarboxylate coordinate to the Cd(II) ions in monodentate and chelating modes, but the bmi ligands with a bridging mode. The IR spectra, PXRD patterns, thermogravimetric analyses, and fluorescence properties are also presented.

Key words: 1-((Benzotriazol-1-yl)methyl)-1*H*-1,3-imidazole, 1,3-Benzenedicarboxylate, Crystal Structure, Fluorescence, Thermogravimetric Analysis, Cobalt(II), Cadmium(II)

Introduction

Metal-organic frameworks (MOFs) with novel topologies and special applications have attracted more and more attention, and much research work has focused on the optimum design of ligands and the rational choice of metals [1 – 3]. Aromatic polycarboxylates such as benzenedicarboxylate, benzenetricarboxylate, benzenetetracarboxylate, and biphenyltetracarboxylate have been demonstrated to be powerful organic ligands, since they have various coordination modes to form diverse structures and can act as hydrogen bonding acceptors and donors in the assembly of supramolecular structures [4 – 8]. On the other hand, flexible multidentate *N*-heterocyclic ligands have also been used widely to construct MOFs with fascinating topologies and useful properties because such ligands often have several potential *N*-donors and can act as both hydrogen bond acceptors and donors, and thus can adopt a variety of conformations according to the restrictions imposed by the coordination requirement of the metal. Until now, a number of MOFs constructed from this kind of ligands have been reported, including both interpenetrating and non-interpenetrating frameworks with rich structural diversities [9 – 12].

The employment of mixed ligands is an effective approach for the construction of novel MOFs, and numerous complexes based on *N*-heterocyclic ligands and aromatic polycarboxylates have been reported [13 – 16]. In the literature we found twenty-one metal-organic complexes with one type of organic bmi ligand [17 – 22] but only two complexes, $[Cu(2,5\text{-pydc})(bmi)(H_2O)]_n$ and $[Cu(btc)_2(bmi)_2]\cdot 1.5H_2O$ (bmi = 1-((benzotriazol-1-yl)methyl)-1*H*-1,3-imidazole, 2,5-H_2pydc = pyridine-2,5-dicarboxylic acid, H_3btc = 1,3,5-benzenetricarboxylic acid) which were obtained using mixed ligands including bmi and aromatic polycarboxylates [23]. In order to enrich the categories and numbers of complexes with mixed ligands, in this paper, we selected bmi and 1,3-benzenedicarboxylic acid (H_2bdc) as ligands to form mixed ligand complexes by reaction with $Co(NO_3)_2\cdot 6H_2O$ or $Cd(NO_3)_2\cdot 6H_2O$, and were able to obtain the compounds $\{[Co(bmi)_2$

(bdc)(H$_2$O)]·2H$_2$O}$_n$ (**1**) and {[Cd(bmi)(bdc)(H$_2$O)]·DMF}$_n$ (**2**). Their structures have been characterized by single-crystal X-ray diffraction, and their luminescence properties and thermogravimetric features have been investigated.

Experimental Section

General information and materials

All chemicals were purchased of AR grade and used without further purification. 1-((Benzotriazol-1-yl)methyl)-1*H*-1,3-imidazole (bmi) was synthesized according to the literature [24]. The IR spectra were obtained on a Bruker Tensor 27 spectrophotometer with KBr pellets in the rage of 400 – 4000 cm^{-1}. Elemental analyses (C, H, and N) were performed on a Flash EA 1112 elemental analyzer. The PXRD patterns were recorded using CuK_α radiation on a PANalytical X'Pert PRO diffractometer. Solid-state luminescence spectra were recorded with a Fluoro Max-P fluorescence spectrophotometer. TG measurements were performed by heating the sample from 30 to 600 °C (or 700 °C for **2**) at 10 °C min^{-1} in air on a Netzsch Sta 409 PC/PG differential thermal analyzer.

*Synthesis of {[Co(bmi)$_2$(bdc)(H$_2$O)]·2H$_2$O}$_n$ (**1**)*

A mixture of Co(NO$_3$)$_2$·6H$_2$O (0.1 mmol), bmi (0.2 mmol), H$_2$bdc (0.1 mmol), DMF (1 mL), methanol (2 mL), and water (5 mL) was placed in a 25 mL Teflon-lined stainless-steel vessel and heated at 80 °C for 72 h. The autoclave was cooled to room temperature at a rate of 10 °C·h^{-1}. Red block-shaped crystals of {[Co(bmi)$_2$(bdc)(H$_2$O)]·2H$_2$O}$_n$ suitable for X-ray analysis were collected. Yield: 52 %. – Anal. for C$_{28}$H$_{28}$CoN$_{10}$O$_7$ (675.53): calcd. C 49.78, H 4.18, N 20.73; found C 50.09, H 4.06, N 20.38. – FT-IR (KBr, cm^{-1}): ν = 3424 (s), 3113 (m), 1603 (s), 1539 (s), 1453 (m), 1380 (s), 1276 (s), 1137 (s), 1101 (s), 1080 (s), 777 (s), 745 (s), 661 (m), 432 (w).

*Synthesis of {[Cd(bmi)(bdc)(H$_2$O)]·DMF}$_n$ (**2**)*

The synthesis of **2** was the same as that for **1**, except that Cd(NO$_3$)$_2$·6H$_2$O (0.1 mmol) was used instead of Co(NO$_3$)$_2$·6H$_2$O. Crystals of {[Cd(bmi)(bdc)(H$_2$O)]·DMF}$_n$ suitable for X-ray analysis were obtained. Yield: 61 %. – Anal. for C$_{21}$H$_{22}$CdN$_6$O$_6$ (566.86): calcd. C 44.36, H 3.90, N 14.78; found C 44.62, H 3.81, N 14.60. – FT-IR (KBr, cm^{-1}): ν = 3423 (s), 3122 (m), 3012 (m), 1667 (s), 1610 (s), 1548 (s), 1453 (m), 1440 (m), 1392 (s), 1228 (s), 1090 (s), 785 (s), 768 (s), 743 (s), 656 (s), 429 (m).

Single-crystal structure determinations

Single crystals were carefully selected and attached to thin glass fibers. Crystal structure determinations were performed on a Rigaku Saturn 724 CCD diffractometer equipped with a graphite monochromator for the X-ray source (MoK_α radiation, λ = 0.71073 Å) operating at 50 kV and 40 mA. The

Table 1. Crystallographic data, data collection and structure refinement details for **1** and **2**.

Complex	**1**	**2**
Empirical formula	C$_{28}$H$_{28}$CoN$_{10}$O$_7$	C$_{21}$H$_{22}$CdN$_6$O$_6$
Formula weight	675.53	566.86
Temperature, K	293(2)	293(2)
Crystal size, mm^3	0.18 × 0.12 × 0.10	0.21 × 0.20 × 0.18
Crystal system	triclinic	monoclinic
Space group	$P\bar{1}$	$P2_1/c$
a, Å	10.242(2)	10.118(2)
b, Å	12.286(3)	11.626(2)
c, Å	13.419(3)	20.055(4)
α, deg	63.31(3)	90
β, deg	88.35(3)	97.10(3)
γ, deg	74.48(3)	90
Volume, Å^3	1445.4(5)	2341.0(8)
Z	2	4
Calculated density, g cm^{-3}	1.55	1.61
Absorption coefficient, mm^{-1}	0.7	1.0
F(000), e	698	1144
θ range for data collection, deg	2.40 → 25.50	2.68 → 27.89
hkl range	±12, ±14, ±16	−12 → 13, ±15, −26 → 15
Reflections collected/unique/R_{int}	15 352/5374/0.0378	14 764/5532/0.0278
Data/ref. parameters	5374/415	5532/309
Goodness-of-fit on F^2	1.122	1.106
Final indices $R1/wR2$ [$I > 2\,\sigma(I)$]	0.0568/0.1293	0.0410/0.0862
Final indices $R1/wR2$ (all data)	0.0684/0.1362	0.0490/0.0908
$\Delta\rho$fin (max/min), e Å^{-3}	0.52/−0.56	0.61/−0.41

Table 2. Selected bond lengths (Å) and angles (deg) for **1** and **2** with estimated standard deviations in parentheses[a].

Complex **1**			
Co1–O3$^{\#1}$	2.042(2)	Co1–O5	2.132(2)
Co1–N1	2.135(3)	Co1–O2	2.145(2)
Co1–N6	2.146(3)	Co1–O1	2.210(2)
O3$^{\#1}$–Co1–O5	95.11(10)	O3$^{\#1}$–Co1–N1	90.09(11)
O5–Co1–N1	90.25(10)	O3$^{\#1}$–Co1–O2	162.13(9)
O5–Co1–O2	102.73(9)	N1–Co1–O2	88.72(10)
O3$^{\#1}$–Co1–N6	91.16(11)	O5–Co1–N6	89.04(10)
N1–Co1–N6	178.62(10)	O2–Co1–N6	90.28(10)
O3$^{\#1}$–Co1–O1	101.65(9)	O5–Co1–O1	163.03(8)
N1–Co1–O1	87.13(10)	O2–Co1–O1	60.47(8)
N6–Co1–O1	93.20(10)		
Complex **2**			
Cd1–O1	2.229(2)	Cd1–N1$^{\#1}$	2.286(3)
Cd1–O4$^{\#2}$	2.331(2)	Cd1–O5	2.353(2)
Cd1–N5	2.360(2)	Cd1–O3$^{\#2}$	2.530(3)
O1–Cd1–N1$^{\#1}$	96.07(10)	O1–Cd1–O4$^{\#2}$	133.34(8)
N1$^{\#1}$–Cd1–O4$^{\#2}$	93.13(10)	O1–Cd1–O5	86.88(8)
N1$^{\#1}$–Cd1–O5	172.26(8)	O4$^{\#2}$–Cd1–O5	90.00(9)
O1–Cd1–N5	138.92(9)	N1$^{\#1}$–Cd1–N5	87.84(9)
O4$^{\#2}$–Cd1–N5	86.95(9)	O5–Cd1–N5	85.25(7)
O1–Cd1–O3$^{\#2}$	80.08(8)	N1$^{\#1}$–Cd1–O3$^{\#2}$	96.54(9)
O4$^{\#2}$–Cd1–O3$^{\#2}$	53.41(8)	O5–Cd1–O3$^{\#2}$	91.01(8)
N5–Cd1–O3$^{\#2}$	140.23(8)		

[a] Symmetry transformations used to generate equivalent atoms: **1**: $^{\#1}$ $x+1, y, z$; **2**: $^{\#1}$ $-x, y-1/2, -z+1/2$; $^{\#2}$ $x-1, y, z$.

data were collected by an ω scan mode at a temperature of 293(2) K. The crystal-to-detector distance was 45 mm. Empirical absorption corrections were applied. The data were corrected for Lorentz and polarization effects. The structures were solved by Direct Methods and refined by full-matrix least-squares on F^2, using the SHELXS/L-97 program package [25]. Hydrogen atoms bound to carbon atoms were placed in calculated positions. The hydrogen atoms of the water molecules were found at reasonable positions in difference Fourier maps. Final refinement included atomic positions for all atoms, anisotropic displacement parameters for all non-hydrogen atoms, and isotropic displacement parameters for all hydrogen atoms. Crystallographic parameters and structure refinement data are summarized in Table 1. Selected bond lengths and bond angles are listed in Table 2 and hydrogen bond parameters in Table 3.

Table 3. Hydrogen bonds of complexes **1** and **2**[a].

D–H···A	*d*(D–H) (Å)	*d*(H···A) (Å)	*d*(D···A) (Å)	(D–H···A) (deg)
Complex **1**				
O6–H4W···N5	0.85	2.13	2.967(4)	168.3
O7–H6W···O2	0.85	1.85	2.695(8)	174.2
O5–H1W···O4$^{\#1}$	0.85	1.87	2.698(3)	164.5
O5–H2W···O6$^{\#4}$	0.85	1.95	2.785(4)	167.4
O6–H3W···O4$^{\#5}$	0.85	2.03	2.866(4)	169.4
O7–H5W···O6$^{\#6}$	0.85	2.54	3.202(15)	158.1
Complex **2**				
O5–H1W···O3$^{\#6}$	0.85	1.98	2.747(3)	148.9
O5–H2W···O1$^{\#5}$	0.85	1.84	2.650(3)	158.2

[a] Symmetry transformations used to generate equivalent atoms: **1**: $^{\#1}$ $x+1, y, z$; $^{\#4}$ $-x+2, -y, -z$; $^{\#5}$ $x+1, y-1, z$; $^{\#6}$ $x-1, y+1, z$; **2**: $^{\#5}$ $-x, -y, -z$; $^{\#6}$ $-x+1, -y, -z$.

CCDC 967184 (**1**) and 967185 (**2**) contain the supplementary crystallographic data for this paper. These data can be obtained free of charge from The Cambridge Crystallographic Data Centre *via* http://www.ccdc.cam.ac.uk/data_request/cif.

Results and Discussion

*IR spectroscopy of complexes **1** and **2***

The IR spectra of complexes **1** and **2** show the absorption bands at 3424 cm^{-1} for **1** and 3423 cm^{-1} for **2** that can be attributed to the stretching vibrations of O–H. The absorption bands at 3113 cm^{-1} for **1** and 3122 cm^{-1} for **2** originate from Ar-H stretching vibrations. The absorption bands at 1603, 1539, 1453 cm^{-1} for **1** and 1610, 1548, 1453 cm^{-1} for **2** correspond to the characteristic stretching vibrations of C=C, N=N and C=N. The absorption bands at 745 cm^{-1} for **1** and 743 cm^{-1} for **2** belong to the characteristic bending vibration of the external 1,2-disubstituted phenyl ring. The absorption bands at 777 cm^{-1} for **1** and 785 cm^{-1} for **2** correspond to characteristic bending vibration of the 1,3-disubstituted phenyl ring. Separations (Δ) between ν_{as} (COO) and ν_s (COO) are different for monodentate, chelating and bridging carboxylates [26]. In complex **1**, these separations are 223 cm^{-1} (1603 and 1380 cm^{-1}) and 86 cm^{-1} (1539 and 1453 cm^{-1}), respectively. In complex **2**, they are 218 cm^{-1} (1610 and 1392 cm^{-1}) and 95 cm^{-1} (1548 and 1453 cm^{-1}), respectively. Therefore, the carboxylate groups in complexes **1** and **2** coordinate to the central metal ions with monodentate and chelating modes. These findings are confirmed by the results of the X-ray diffraction.

*Crystal structure of {[Co(bmi)$_2$(bdc)(H$_2$O)]·2H$_2$O}$_n$ (**1**)*

Single-crystal X-ray diffraction has revealed that complex **1** crystallizes in the triclinic system in space

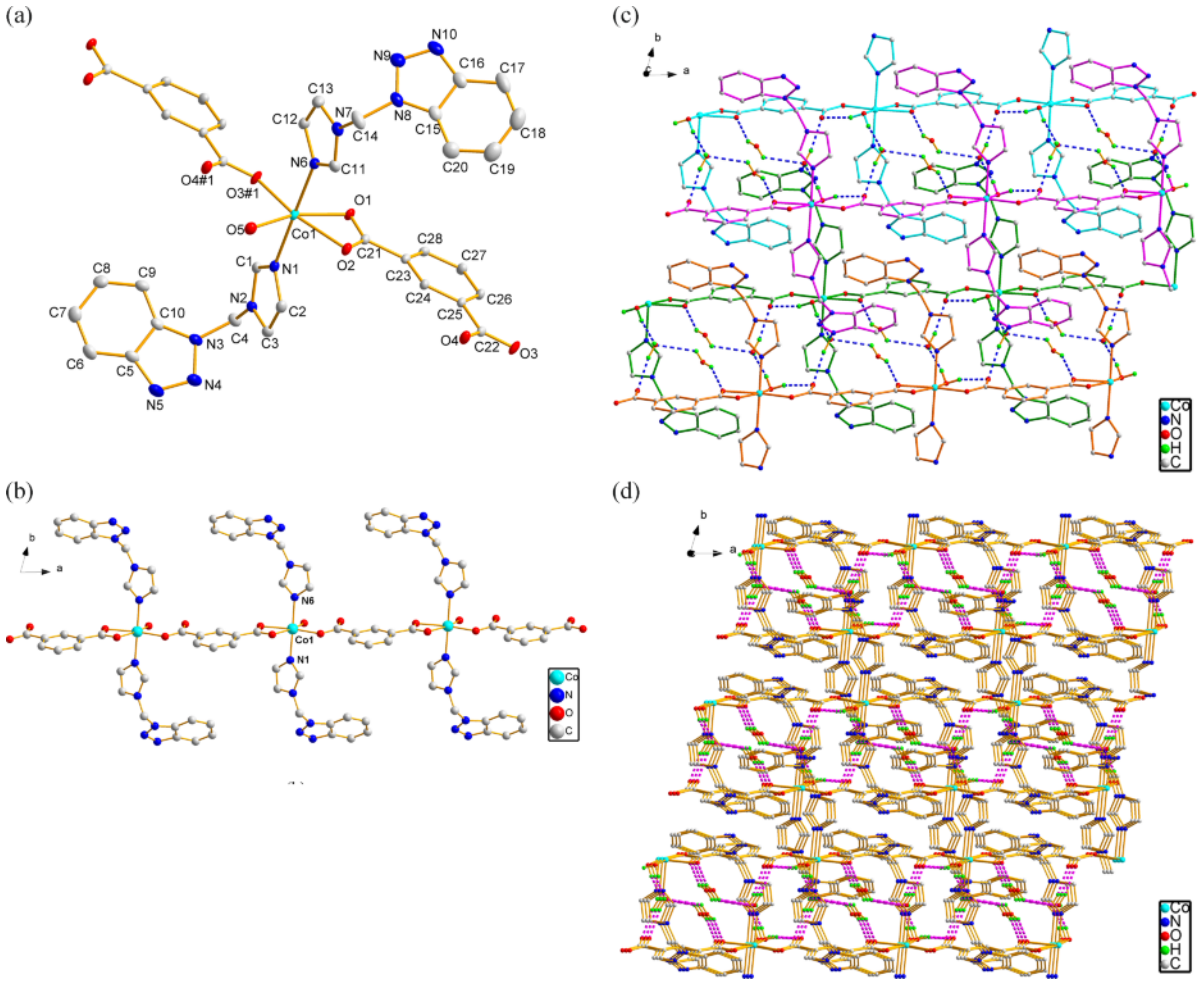

Fig. 1 (color online). (a) Coordination environment of the Co(II) ion in complex **1** with ellipsoids drawn at the 20 % probability level; hydrogen atoms and uncoordinated water molecules are omitted for clarity ($^{\#1}$ $x+1, y, z$); (b) view of the chain structure of complex **1**; (c) view of the layer structure of complex **1** linked through hydrogen bonds indicated by dashed lines and π-π interactions; (d) 3-D structure of complex **1**.

group $P\bar{1}$, and there are one Co(II) ion, two bmi ligands, one 1,3-benzenedicarboxylate anion, one coordinated and two uncoordinated water molecules in each asymmetric unit. As shown in Fig. 1a, each Co(II) ion is hexacoordinated by three oxygen atoms belonging to one chelating carboxylate group and one monodentate carboxylate group of two symmetry-related 1,3-benzenedicarboxylates, two nitrogen atoms from two crystallographically independent bmi ligands and one coordinated water molecule. Atoms O1, O2, O3$^{\#1}$, O5, and Co1 which are nearly coplanar (the mean deviation from plane is 0.0181 Å, symmetry codes: $^{\#1}$ $x+1$, y, z) complete the equatorial plane, while the apical positions are occupied by N1 and N6 with the N1–Co1–N6 bond angle of 178.6(1)°. Therefore, the local environment around Co1 can be described as a distorted octahedron. The Co–O bond lengths range from 2.042(2) to 2.210(2) Å, and the Co–N bond lengths are 2.135(3) and 2.146(3) Å. These Cd–O and Cd–N bond lengths are close to those in the reported Co(II) complexes $[Co(bmi)_2(NO_3)_2]_n$ [17], $\{[Co(OOC(CH_2)_3Fc)(\eta^2\text{-}OOC(CH_2)_3Fc)(bbbm)]\cdot CH_3OH\}_n$ (Fc = $(\eta^5\text{-}C_5H_5)Fe(\eta^5\text{-}C_5H_4)$, bbbm = 1,1-(1,4-butanediyl)bis-1*H*-benzimidazole) [27], and $[Co_4(TPOM)_2(bdc)_4(H_2O)_4]\cdot H_2O$ (TPOM = tetrakis(4-pyridyloxymethylene)methane) [28].

As is shown in Fig. 1b, the 1,3-benzenedicarboxylic acid is fully deprotonated, and the dihedral angles between the mean plane defined by the benzene ring and the chelating and monodentately coordinated carboxylate groups are *ca*. 5.0 and 3.0°, respectively. Each bdc^{2-} anion bridges two Co(II) ions to form a chain *via* Co–O bonds in the chelating and monodentate modes. The chain extends along the crystallographic *a* directon, all Co(II) ions in one chain are strictly on one line, and the intrachain Co···Co distance separated by a bdc^{2-} unit is *ca*. 10.2 Å. In complex **1**, there are two crystallographically independent bmi ligands. One kind (containing the N1 atom) with a dihedral angle of *ca*. 112.0° between the benzotriazole and imidazole rings, coordinates to Co(II) ion in monodentate mode and is situated at one side of the main chain. The other kind (containing the N6 atom) with a dihedral angle of *ca*. 118.7° between the benzotriazole and imidazole rings also coordinates to a Co(II) ion in monodentate mode and is situated at the other side of the main chain. As depicted in Table 3 and Fig. 1c, there are five kinds of O–H···O hydrogen bonds between non-coordinated water molecules, between non-coordinated and coordinated water molecules and carboxylate groups, between coordinated and non-coordinated water molecules, and one kind of O–H···N hydrogen bonds between solvent water molecules and benzotriazole groups. The distance between the benzene rings of benzotriazole units of adjacent chains is *ca*. 3.5 Å, and the distance between the benzene rings of 1,3-benzenedicarboxylates of adjacent chains is *ca*. 3.2 Å. The chains are linked by the above six kinds of hydrogen bonds and by π-π interactions leading to layers parallel to the *ab* plane. The layers are further stacked through intermolecular forces giving a 3-D packing structure in the solid state (Fig. 1d).

Crystal structure of $\{[Cd(bmi)(bdc)(H_2O)]\cdot DMF\}_n$ *(**2**)*

Because the structures of complexes can be influenced by various factors including the metal centers [27], we introduced Cd(II) to the reaction system with other experimental conditions unchanged and obtained compound **2**. The structure determination has revealed that **2** crystallizes in the monoclinic system with space group $P2_1/c$. The asymmetric unit contains one Cd(II) ion, one bmi ligand, one 1,3-benzenedicarboxylate anion, one coordinated water molecule, and one uncoordinated DMF molecule. As is depicted in Fig. 2a, Cd(II) is six-coordinate with a distorted octahedral geometry by one monodentate carboxylate oxygen atom and two chelating carboxylate oxygen atoms from two symmetry-related 1,3-benzenedicarboxylates, two nitrogen atoms from two symmetry-related bmi ligands and one coordinated water molecule. Atoms O1, $O3^{\#2}$, $O4^{\#2}$, N5 and Cd1 occupy the equatorial positions (the mean deviation from the plane is 0.0337 Å), and atoms $N1^{\#1}$ and O5 are located in the apical positions with the $N1^{\#1}$–Cd1–O5 bond angle of 172.26(8)° (symmetry codes: $^{\#1}$ $-x,\ y-1/2,\ -z+1/2$; $^{\#2}$ $x-1,\ y,\ z$). The Cd–O bond lengths are in the range 2.229(2) – 2.530(3) Å, and the Cd–N bond lengths are 2.286(3) and 2.360(2) Å. They are similar to those of other Cd(II) complexes $[Cd(bpy)(bdp)(H_2O)]_n$, $Cd(bpy)(btec)_{1/2}(H_2O)]_n$, ($H_2bdp$ = 1,4-benzenedicarboxylic acid, H_4btec = 1,2,4,5-benzenetetracarboxylic acid, bpy = 2,2′-bipyridine) and $\{[Cd(bdc)(tmb)(H_2O)]\cdot CH_3OH\}_n$ (tmb = 2-((1*H*-1,2,4-triazol-1-yl)methyl)-1*H*-benzimidazole) [29, 30].

Similar to complex **1**, the 1,3-benzenedicarboxylic acids are fully deprotonated, but the conformation of the anions in **2** is different from that in **1**. In complex **2**, the dihedral angle between the mean plane defined by the benzene ring and the chelating and monodentately coordinated carboxylate groups are *ca*. 5.7 and 8.6°, which are larger than those in complex **1**. As is shown in Fig. 2b, each bdc^{2-} anion bridges two Cd(II) ions to form a chain *via* Cd–O bonds in chelating and monodentate coordination modes. The chain extends along the *a* directon with all of the Cd(II) ions in one chain being strictly on a line, and the intrachain Cd···Cd distance separated by a bdc^{2-} group is *ca*. 10.1 Å. In addition, also different from **1**, all of the bmi ligands in **2** are crystallographically equivalent and coordinate to Cd(II) ions in bridging mode. The dihedral angle between the benzotriazole and imidazole rings is *ca*. 101.7°. The Cd(II) ions bridged by the bmi ligands generate another linear chain along the *b* direction with the intrachain Cd···Cd distance of *ca*. 8.5 Å. The chains along the two directions are interconnected to give a 2-D framework. We also found that benzotriazole rings between adjacent layers are arranged in parallel fashion with the interplanar distance of *ca*. 3.3 Å, and the benzene rings of 1,3-benzenedicarboxylates between adjacent layers are stacked in parallel fashion with the

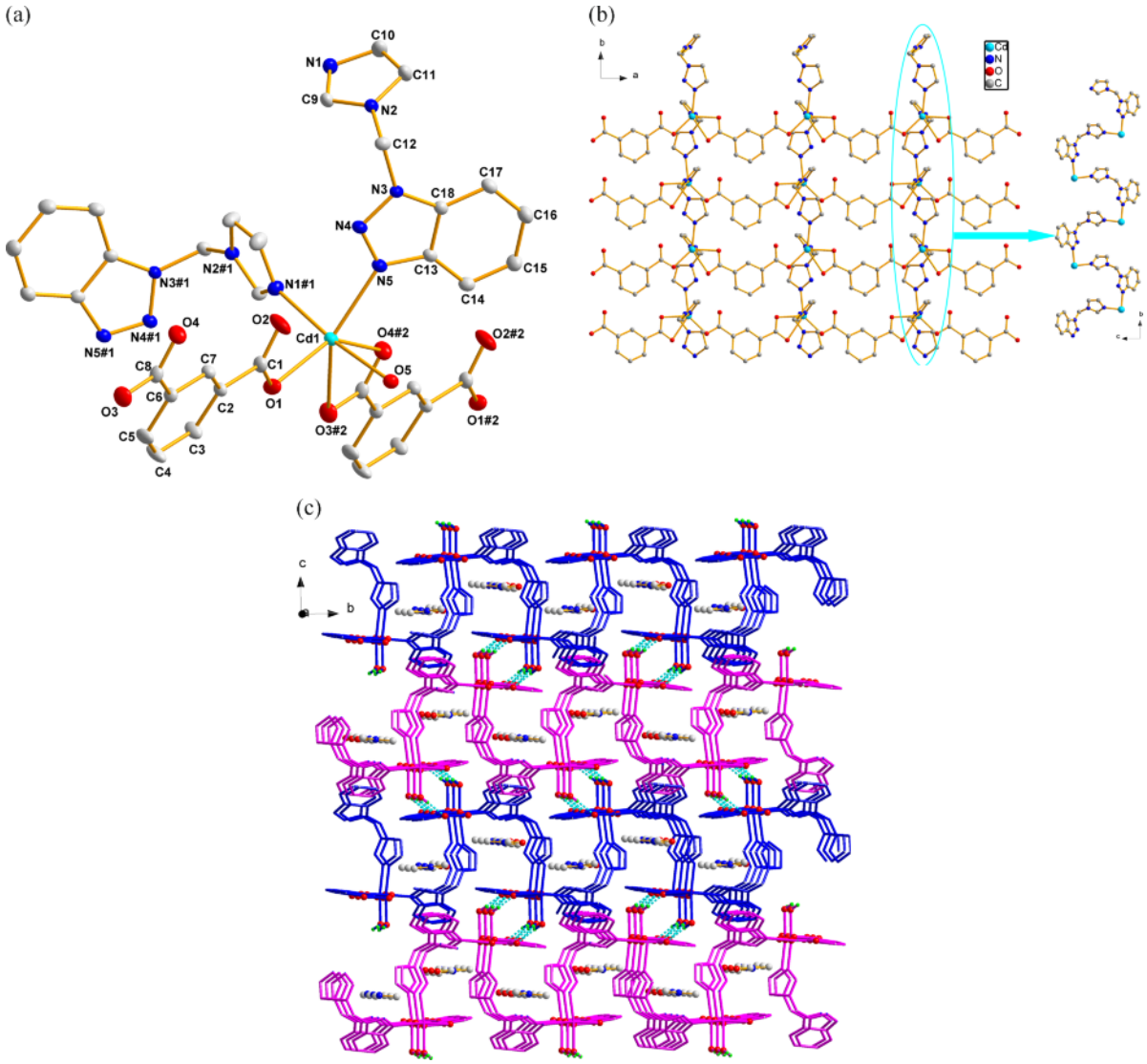

Fig. 2 (color online). (a) Coordination environment of the Cd(II) ion in complex **2** with ellipsoids drawn at the 20 % probability level, hydrogen atoms and uncoordinated DMF molecules are omitted for clarity ($^{\#1}$ $-x$, $y-1/2$, $-z+1/2$; $^{\#2}$ $x-1$, y, z.); (b) the layer structure of complex **2**; part of the benzene rings are omitted for clarity; (c) 3-D structure of complex **2** linked through hydrogen bonds indicated by dashed lines and π-π interactions.

interplanar distance of *ca*. 3.7 Å. Furthermore, there are two kinds of O–H···O hydrogen bonds between coordinated water molecules and carboxylate groups. Adjacent layers are connected by these O.−H···O hydrogen bonds and π-π interactions leading to a 3-D structure in the solid state (Fig. 2c). DMF molecules co-crystallize with complex **2**, but do not coordinate to Cd(II) or form hydrogen bonds with the complex.

XRD patterns

To confirm the phase purity of the two complexes, powder X-ray diffraction patterns (Fig. 3) were recorded for **1** and **2**, and they are comparable to the corresponding simulated ones calculated from the single-crystal diffraction data, indicating a pure phase of each bulk sample.

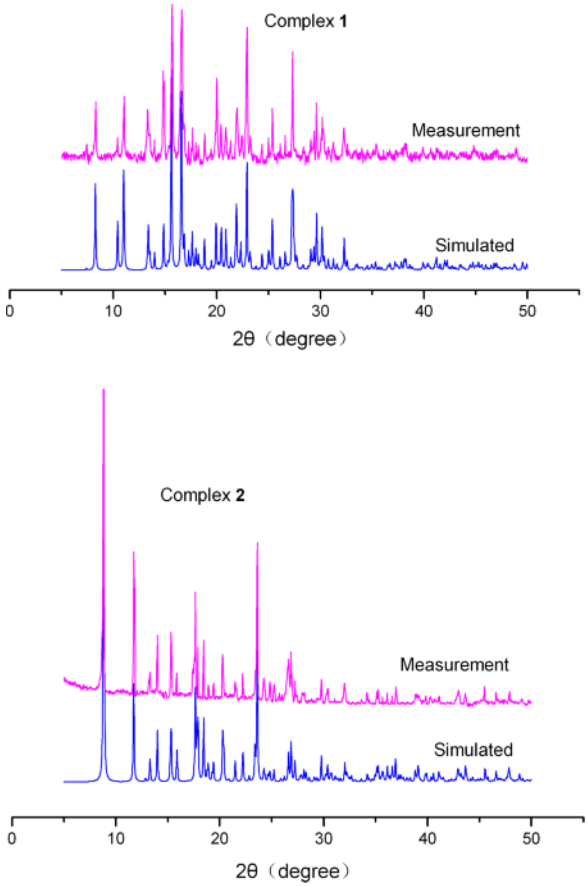

Fig. 3 (color online). The PXRD patterns of complexes **1** and **2** at room temperature.

Thermogravimetric analysis

Thermogravimetric analyses of complexes **1** and **2** were performed by heating the complexes from 30 to 600 °C (700 °C for **2**) in air. As is shown in Fig. 4, the TG curve of **1** exhibits the first mass loss of 7.8 % between 68 to 143 °C, corresponding to the release of the solvent and coordination water molecules (calcd. 8.0 %). Then the solid continues to lose mass from 238 to 487 °C, corresponding to the decomposition of bmi ligands and 1,3-benzenedicarboxylates. Finally, a plateau occurs from 487 to 600 °C. The residue equals 10.9 %, which is attributed to CoO (calcd. 11.1 %). The TG curve of complex **2** reveals a weight loss of 15.8 % from 108 to 208 °C, which can be assigned to the release of coordinated water molecules as well as solvent DMF molecules (calcd.

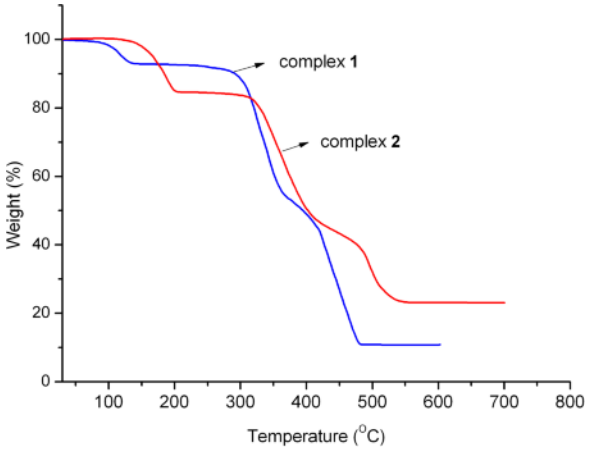

Fig. 4 (color online). TG curves of complexes **1** and **2**.

16.1 %). Continuous weight loss from 285 to 562 °C corresponds to the decomposition of bmi ligands and 1,3-benzenedicarboxylates. A plateau is observed from 562 to 700 °C. The residue of 23.0 % appears to be CdO (calcd. 22.7 %). All these results are in agreement with the aforementioned crystal structure.

Luminescence properties

The fluorescence properties of **1** and **2** were determined in solid state at room temperature. As is shown in Fig. 5, complex **2** exhibits an emission peak with a maximum at 345 nm upon excitation at 308 nm, but no clear photoluminescence was observed for complex

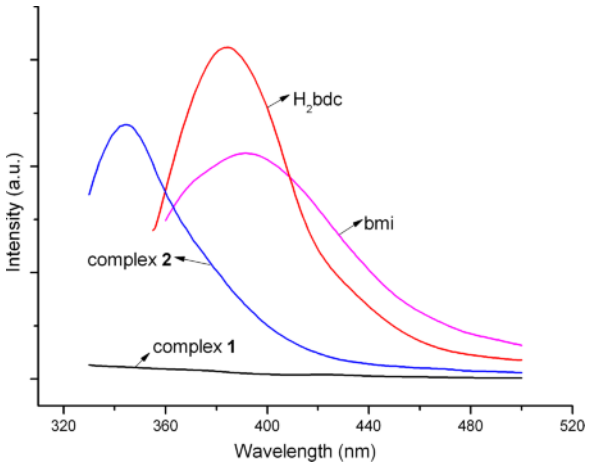

Fig. 5 (color online). Solid-state emission spectra of bmi, H$_2$bdc and complexes **1** and **2**.

1. To further analyze the nature of the emission band, the luminescence properties of free bmi and H_2bdc have also been investigated. The uncoordinated bmi ligand fluoresces in the solid state with a main emission peak at 392 nm upon excitation at 339 nm, and H_2bdc exhibits a band with an emission maximum at 384 nm upon excitation at 345 nm. Thus it could be assumed that both the nitrogen-donor and oxygen-donor contribute to the fluorescence of complex **2** simultaneously. In comparison with the bands for uncoordinated bmi and H_2bdc, the emission spectrum for complex **2** appears blueshifted. This could be assigned to the coordination of Cd(II) ions to the bmi and bdc^{2-} ligands and to hydrogen bonding, which increase the rigidity of the complex and reduce the loss of energy by radiationless decay of the intraligand emission from excited states [31 – 34]. The emission intensity for **1** is weak, and this can be attributed to the fluorescence quenching effect caused by Co(II) [35]. This consequence further confirms the conclusion that complexes constructed from d^{10} metal centers and conjugated organic linkers are promising candidates for photoactive materials [36]. Replacing the metal center could be a way to adjust the fluorescence intensity of the products.

Conclusion

The compounds $\{[Co(bmi)_2(bdc)(H_2O)]\cdot 2H_2O\}_n$ (**1**) and $\{[Cd(bmi)(bdc)(H_2O)]\cdot DMF\}_n$ (**2**) have been isolated from the reactions of imb and H_2bdc with $Co(NO_3)_2\cdot 6H_2O$ or $Cd(NO_3)_2\cdot 6H_2O$. The results suggest that the combination of *N*-heterocyclic ligands and aromatic polycarboxylates with suitable metal centers might be a promising strategy for the construction of MOFs with a specific structure and topology. This work has shown that the change of metal ions influences the coordination modes of bmi ligands, and thus influences the detailed architectures of the complexes, and finally leads to different photophysical properties.

Acknowledgement

We gratefully acknowledge the financial support by the National Natural Science Foundation of China (no. J1210060).

[1] M. Wriedt, A. A. Yakovenko, G. J. Halder, A. V. Prosvirin, K. R. Dunbar, H. C. Zhou, *J. Am. Chem. Soc.* **2013**, *135*, 4040.
[2] B. A. Blight, R. Guillet-Nicolas, F. Kleitz, R. Y. Wang, S. N. Wang, *Inorg. Chem.* **2013**, *52*, 1673.
[3] K. P. Rao, M. Higuchi, J. G. Duan, S. Kitagawa, *Cryst. Growth Des.* **2013**, *13*, 981.
[4] L. Gao, B. J. Zhao, G. H. Li, Z. Shi, S. H. Feng, *Inorg. Chem. Commun.* **2003**, *6*, 1249.
[5] Q. R. Fang, G. S. Zhu, X. Shi, G. Wu, G. Tian, R. W. Wang, S. L. Qiu, *J. Solid State Chem.* **2004**, *177*, 1060.
[6] J. Fan, H. F. Zhu, T. A. Okamura, W. Y. Sun, W. X. Tang, N. Ueyama, *New J. Chem.* **2003**, *27*, 1409.
[7] O. Fabelo, J. Pasán, L. Cañadillas-Delgado, F. S. Delgado, A. Labrador, F. Lloret, M. Julve, C. Ruiz-Pèrez, *Cryst. Growth Des.* **2008**, *8*, 3984.
[8] S. Guo, D. Tian, Y. Luo, H. Zhang, *J. Coord. Chem.* **2012**, *65*, 308.
[9] H. Wu, J. Yang, Y. Y. Liu, J. F. Ma, *Cryst. Growth Des.* **2012**, *12*, 2272.
[10] K. Biradha, A. Mondal, B. Moulton, M. J. Zaworotko, *J. Chem. Soc., Dalton Trans.* **2000**, 3837.
[11] X. R. Meng, Y. L. Song, H. W. Hou, H. Y. Han, B. Xiao, Y. Y. Fan, Y, Zhu, *Inorg. Chem.* **2004**, *43*, 3528.
[12] J. P. Zhang, Y. Y. Lin, W. X. Zhang, X. M. Chen, *J. Am. Chem. Soc.* **2005**, *127*, 14162.
[13] X. Su, T. Li, Y. Xiu, X. R. Meng, *Z. Naturforsch.* **2012**, *67b*, 678.
[14] G. H. Jin, Y. Yang, X. L. Zhou, X. R. Meng, *Z. Naturforsch.* **2012**, *67b*, 29.
[15] K. M. Blake, C. M. Gandolfo, J. W. Uebler, R. L. LaDuca, *Cryst. Growth Des.* **2012**, *12*, 5125.
[16] L. Qin, J. S. Hu, M. D. Zhang, Y. Z. Li, H. G. Zheng, *Cryst. Growth Des.* **2012**, *12*, 4911.
[17] X. R. Meng, X. Q. Zhu, Y. F. Qi, H. W. Hou, Y. T. Fan, *J. Mol. Struct.* **2009**, *934*, 28.
[18] L. K. Duan, Y. N. Ding, X. R. Meng, W. Q. Li, H. W. Hou, Y. T. Fan, *J. Mol. Struct.* **2010**, *975*, 53.
[19] L. K. Duan, S. L. Liu, W. Zhou, X. R. Meng, *Synth. React. Inorg. Met.-Org. Chem.* **2010**, *40*, 319.
[20] Y. Wang, Y. Y. Sun, *Acta Crystallogr.* **2011**, *E67*, m920.
[21] X. L. Zhou, W. Q. Li, G. H. Jin, D. Zhao, X. Q. Zhu, X. R. Meng, H. W. Hou, *J. Mol. Struct.* **2011**, *995*, 148.
[22] C. X. An, X. L. Han, P. B. Wang, Z. H. Zhang, H. K. Zhang, Z. J. Fan, *Trans. Met. Chem.* **2008**, *33*, 835.
[23] J. Y. Hu, C. L. Liao, J. A. Zhao, *J. Chem. Res.* **2012**, *36*, 413.
[24] A. R. Katritzky, M. Drewniak-Deyrup, X. Lan, F. Brunner, *J. Heterocycl. Chem.* **1989**, *26*, 829.
[25] G. M. Sheldrick, *Acta Crystallogr.* **2008**, *A64*, 112.

[26] K. Nakamoto, *Infrared and raman spectra of inorganic and coordination compounds*. Part B, 6th ed., John Wiley, Hoboken, New Jersey, **2009**, pp. 64.
[27] X. R. Meng, W. Zhou, Y. F. Qi, H. W. Hou, Y. T. Fan, *J. Organomet. Chem.* **2010**, *695*, 766.
[28] J. Guo, J. F. Ma, B. Liu, W. Q. Kan, J. Yang, *Cryst. Growth Des.* **2011**, *11*, 3609.
[29] R. Prajapati, L. Mishra, K. Kimura, P. Raghavaiah, *Polyhedron* **2009**, *28*, 600.
[30] X. X. Wang, X. Han, Z. Qiao, G. H. Jin, X. R. Meng, *Z. Naturforsch.* **2012**, *67b*, 783.
[31] P. K. Chen, Y. X. Che, Y. M. Li, J. M. Zheng, *J. Solid State Chem.* **2006**, *179*, 2656.
[32] Y. F. Zhou, B. Y. Lou, D. Q. Yuan, Y. Q. Xu, F. L. Jiang, M. C. Hong, *Inorg. Chim. Acta* **2005**, *358*, 3057.
[33] N. W. Alcock, P. R. Barker, J. M. Haider, M. J. Hannon, C. L. Painting, Z. Pikramenou, E. A. Plummer, K. Rissanen, P. Saarenketo, *J. Chem. Soc., Dalton Trans.* **2000**, 1447.
[34] V. W. W. Yam, K. K. W. Lo, *Chem. Soc. Rev.* **1999**, *28*, 323.
[35] W. L. Liu, L. H. Ye, X. F. Liu, L. M. Yuan, J. X. Jiang, C. G. Yan, *CrystEngComm* **2008**, *10*, 1395.
[36] B. Ding, L. Yi, Y. Wang, P. Cheng, D. Z. Liao, S. P. Yan, Z. H. Jiang, H. B. Song, H. G. Wang, *Dalton Trans.* **2006**, 665.